Bright and dark walks for dressed-photon–phonon transfer

M. Ohtsu[1], E. Segawa[2], K. Yuki[3], and S. Saito[4]

[1]Research Origin for Dressed Photon,3-13-19 Moriya-cho, Kanagawa-ku, Yokohama, Kanagawa 221-0022, Japan

[2]Yokohama National University, 79-8 Tokiwadai, Hodogaya-ku, Yokohama, Kanagawa 240-8501, Japan

[3]Middenii, 3-3-13 Nishi-shinjuku, Sinjuku-ku, Tokyo 160-0023, Japan

[4]Kogakuin University, 2665-1, Nakano-machi, Hachioji, Tokyo 192-0015, Japan

Abstract

This paper analyzes the dressed-photon–phonon energy transfer from several nanometer-sized particles for an input signal terminal (NP_I) to that for output signal terminals (NP_O), which are arranged in rotationally symmetric and asymmetric manners. A quantum walk model is used for numerical calculations by assuming a pentagonal wheel arrangement. In the case where the number n_{con} of connected spokes of the wheel is odd, the signal transfer route is a triply degenerate bright walk. In the case where n_{con} is even, this route is decomposed into bright and dark walks. Since some input signals are injected into the dark walk and are confined in this walk, the output signal transfer rate is smaller than that in the case of the odd n_{con}. The degeneracy in the bright walk and confinement in the dark walk are found also in other polygonal arrangements. It was demonstrated that their features are independent of the number of NP_I on the rim of the wheel of these arrangements.

1. Introduction

Theoretical studies on the creation process of dressed photons (DPs) have made striking progress in recent years and have succeeded in drawing an intuitive physical picture based on the concept of Majorana fermions [1,2]. In parallel with these studies, intensive experimental studies have precisely evaluated the intrinsic features of the energy transfer between nanometer-sized particles (NPs) mediated by dressed-photon–phonons (DPPs) for a variety of applications [3,4]. A typical example of such applications is optical-wavelength conversion, which is realized by the DPP energy transfer from a small NP to a large NP [5]. It was confirmed that the optical/electrical energy conversion efficiency of a solar cell battery was increased by utilizing the optical-wavelength conversion realized by dispersing NPs into a resin film and installing the film on the surface of the battery.

The intrinsic characteristics of the DPP energy transfer between these NPs have been analyzed based on a quantum walk (QW) model [6]. The reasons why the QW model was successfully used in these analyses were due to two features that were common to the dynamic properties of the QW model and the DPP energy transfer process: *non-commutativity* and *localization* [7]. Numerical calculations based on the results of these analyses have been carried out in the case where a large NP for the output

signal terminal (NP_O) was surrounded by small NPs for the input signal terminals (NP_Is) in a rotationally symmetric manner [6]. Figure 1(a) schematically illustrates this arrangement, in which NP_O is fixed on a hub at the center of a wheel. NP_Is are fixed on the rim and are connected to each other. They are also connected to NP_O, as represented by spokes. These rim and spokes represent the DPP energy transfer routes. It was confirmed by numerical calculations that the efficiency of the energy transfer from NP_Is to NP_O was the highest when the number of NP_Is was in the range between 4 and 6, which revealed unique autonomous features of the DPP energy transfer.

In order to advance the analyses and discussions on the DPP energy transfer, the present paper reports the results of numerical calculations for the case where the rotational symmetry above is broken.

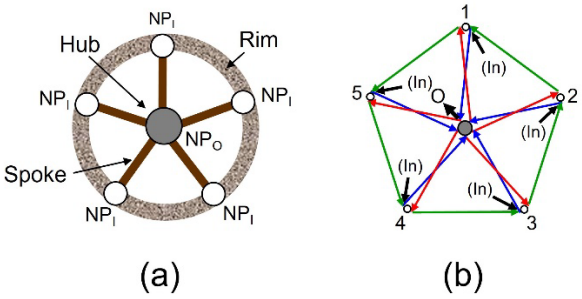

Fig. 1 Rotationally symmetric arrangement of nanometer-sized particles (NPs).

(a) Schematic explanation of a wheel. NP_Is and NP_O are fixed on the rim and on a hub at the center of a wheel, respectively. (b) A pentagonal arrangement of five NP_Is and one NP_O. Five NP_Is on the rim serve as the input signal terminals (ISTs). The NP_O at the hub serves as the output signal terminal (OST). Red and blue arrows represent the directions of signal transfer from and to the hub, respectively. Green arrows represent the transfer direction from one NP_I to the adjacent one on the rim. Short black arrows at the ISTs and OST represent the directions of the input signal injection and output signal transfer, respectively. The symbol **(In)** indicates that the input signal is injected to the ISTs inside the facial closed walk.

2. A quantum walk model

As an example of the broken rotational symmetry, this paper adopts the case in which several spokes between NP_I and NP_O are disconnected. This disconnection is experimentally plausible when the optical properties of the relevant NP_I are deteriorated or the separation between the NP_I and NP_O is extraordinarily large.

Preliminary numerical calculations have been carried out based on the quantum master equations for the creation probabilities of excitons in the NPs [8]. However, since these calculations did not deal with DPP creation probabilities, they were inconsistent with the off-shell science of the theoretical framework of the DPP creation process. Even so, several suggestive results were obtained. One of such results is that, even when several spokes were disconnected, the output signal intensity was as high as, or even higher than that without any disconnections. This reveals that the DPP energy reaches the NP_O by ingeniously detouring via routes to avoid disconnected spokes. This feature

suggests the autonomous features mentioned in Section 1.

In order to compare with the preliminary results above, in the present work we carried out numerical calculations based on the QW model in ref. [6] by assuming that N NP_Is are arranged around NP_O. As was the case of ref. [8], a pentagonal arrangement is dealt with (N=5). The results for tetragonal (N=4) and hexagonal (N=6) arrangements are also presented.

3. Results of numerical calculations

The results of numerical calculations for the pentagonal arrangement elucidated that the value of the output signal transfer rate (OSFR) depended on whether the number n_{con} of connected spokes was odd or even. Sections 3.1 and 3.2 present the results for these two cases. Section 3.3 claims that these features are independent of the total number N of corners of the polygon.

3.1. An odd number n_{con} of connected spokes

a. The case of n_{con}=5

Figure 1(b) shows that five NP_Is are fixed on the rim. They work as the input signal terminals (ISTs). NP_O is fixed at the hub and works as the output signal terminal (OST). Short black arrows connected to these terminals represent the directions of the input signal injection and output signal transfer, respectively. The symbol **(In)** indicates that the input signal is injected to the IST inside the facial closed walk. This figure also shows that the number N_{in} of these input signals is 5, which means that all of the input signals transfer from the IST to the OST and generate the output signal. Thus, the transfer routes in Fig. 1(b) are called a bright walk.

Figure 2(a) shows the results of numerical calculations. The horizontal axis represents the time passed after starting the input signal injection. The curve O is the OSTR that is emitted to the outer space by energy dissipation at the OST. The curves 1–5 are the input signal transfer rates (ISTRs) from the ISTs 1–5 to the OST. This figure shows that the values of the curves 1–5 are different from each other even though the five NP_Is in Fig. 1(b) are arranged in a rotationally symmetric manner. This indicates that the signal transfer features do not reflect the rotational symmetry, which was due to the output signal extraction. That is, the symmetry was broken by adding the short black arrow at the hub.

By comparing the stationary values of curves 1–5 a sufficiently long time after the input signal injection, it is found that the value for curve 1 is the largest, and those of curves 3, 5, 2, and 4 are smaller in this order. The first row of Table 1 summarizes these stationary values. This order depends on the distance of the signal transfer routes to the OST. Since the distance from IST 1 to the OST is the shortest (Fig. 2(b)), the injected signal reaches the OST most efficiently, making the stationary value of the curve 1 the largest. In contrast, since that from IST 4 to the OST is the longest,

the stationary value of curve 4 is the smallest.

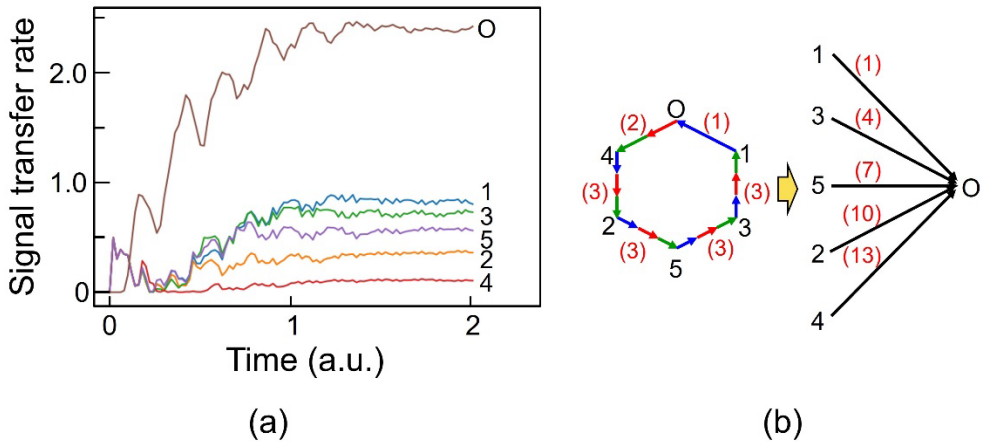

Fig. 2 Results of numerical calculations for the arrangement in Fig. 1(b).

(a) Temporal variations of the input and output signal transfer rates (ISTR and OSTR). Curve O is for the OSTR. Curves 1–5 are for the ISTRs from the ISTs 1–5.

(b) (Left) Number of steps required to transfer from one terminal to the other. They are the numbers of red, blue and green arrows in Fig. 1(b)). (Right) The number in ( ) represents the number of steps that represents the distance from each IST to the OST.

b. The case of n_{con} =3

Figure 3 shows the arrangement for n_{con} =3 in which spokes 1 and 2 are disconnected. It also shows that N_{in} =5, as was the case in Fig. 1(b). That is, all the input signals transfer to the OST and generate the output signal. Thus, the transfer routes in Fig. 3 are also the bright walk. Figure 4(a) shows the results of numerical calculations. The second row of Table 1 summarizes the stationary values for the curves O and 1–5. Since the distance from IST 3 to the OST is the shortest (Fig. 4(b)), the injected signal reaches the OST most efficiently, making the stationary value of the curve 3 the largest. In contrast, since that from IST 4 to the OST is the longest, the stationary value of curve 4 is the smallest. This distance-dependent feature is consistent with that of Fig. 2(b).

The results of numerical calculations for the cases of disconnecting the spokes 1 and 3 and also the spokes 2 and 4 are equal to those in Fig. 4. Their stationary values are given in the third and fourth rows of Table 1, respectively.

By comparing the stationary values of the OSFR on the second-to-fourth rows of Table 1 with that of the first row (n_{con} =5), it is easily found they are equal to each other. Furthermore, the values of the ISFRs are equal in spite of the fact that they change their positions in each row. It is confirmed from these equalities that the walks of n_{con} =5 and 3 are degenerate.

Table 1 Stationary values of the ISFR and OFSR. The number n_{con} of connected spokes is odd (=5,3, and 1).

	n_{con}	The terminal number of disconnected spokes	ISFR					OSFR
			From terminal 1	From terminal 2	From terminal 3	From terminal 4	From terminal 5	
1	5	N.A.	0.834	0.357	0.731	0.108	0.575	2.396
2	3	1,2	0.575	0.357	0.834	0.108	0.731	2.396
3	3	1,3	0.357	0.834	0.731	0.108	0.575	2.396
4	3	2,4	0.834	0.731	0.357	0.108	0.575	2.396
5	1	1,2,3,4	0.731	0.575	0.357	0.108	0.834	2.396

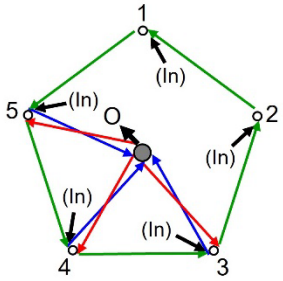

Fig. 3 Arrangement with two disconnected spokes 1 and 2.

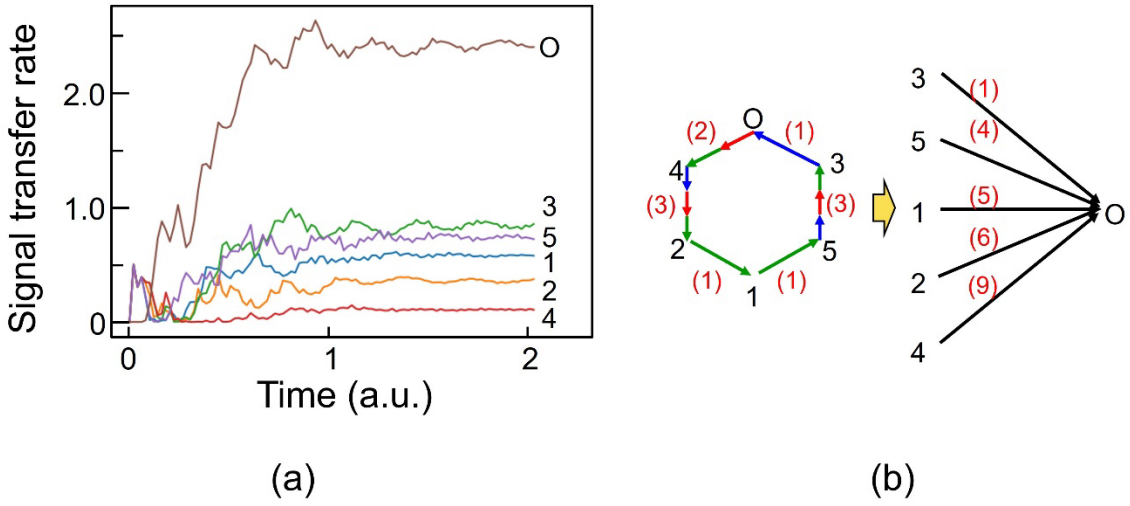

Fig. 4 Results of numerical calculations for the arrangement in Fig. 3.

For captions of (a) and (b), refer to those in Fig. 2.

c. The case of n_{con} =1

Figure 5 shows the arrangement of n_{con} =1 in which only spoke 5 survives. Even so, this figure

represents also N_{in} =5 and thus, the bright walk. Figure 6(a) shows the results of numerical calculations. The fifth row of Table 1 summarizes the stationary values for the curves O and 1–5. This figure and table show that the stationary value of curve 5 is the largest. This distance-dependent feature is consistent with that of Fig. 2(b) because the distance from IST 5 to the OST is the shortest (Fig. 6(b)). For other arrangements of n_{con} =1, numerical calculations gave results that are equal to those of Fig. 6(a). From this equality, it is confirmed that the bright walk of Fig. 5 is degenerate with the bright walks of **a.** (n_{con} =5) and **b.** (n_{con} =3).

To summarize the results of **a.** – **c.** above, all the input signals transfer to the NP_O through the bright walk and generate the output signal. Thus, even if some spokes are disconnected, the stationary values of the OSFR remain unchanged, which means that these bright walks are triply degenerate.

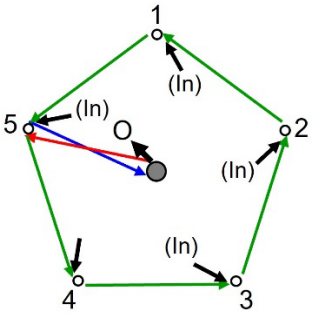

Fig. 5 Arrangement with four disconnected spokes 1–4.

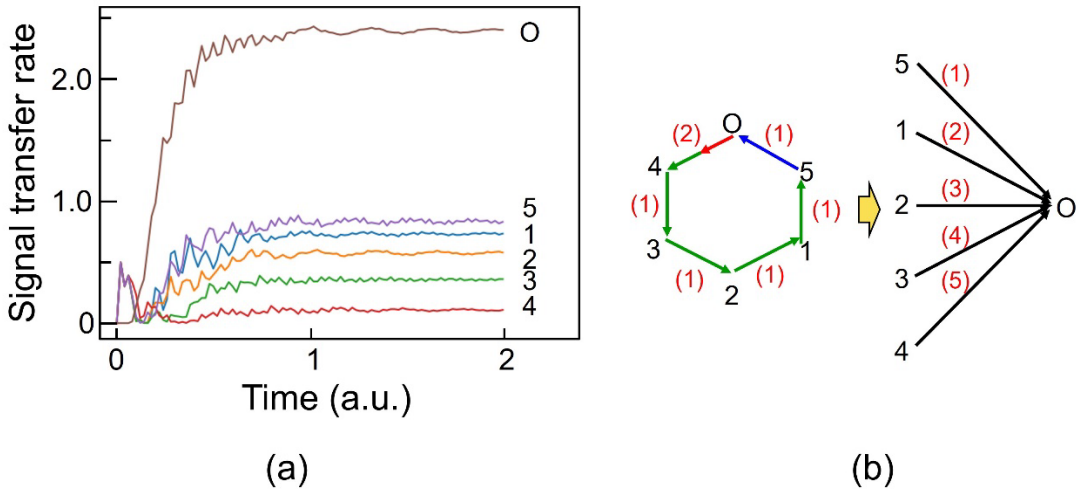

Fig. 6 Results of numerical calculations for the arrangement in Fig. 5.

For captions of (a) and (b), refer to those in Fig. 2.

3.2. An even number n_{con} of connected spokes

a. The case of n_{con} =4

The arrangements have two configurations **(1)** and **(2)** below.

(1) Figure 7(a) schematically illustrates the arrangement of disconnecting the spoke for IST 1, which can be decomposed into two modes (Fig. 7(b))*. Since the red and blue arrows for the transfer routes in Mode 1 contact the short black arrow for the output signal at the hub, the input signal is successfully converted to the output signal at the OST. In Mode 2, on the other hand, since these arrows do not contact the short black arrow at the hub, the input signal fails to be converted to the output signal. Instead, it is confined in the wheel. That is, Mode 2 represents the dark walk, while Mode 1 is the bright walk**.

Because Mode 2 does not generate the output signal, it is sufficient to carry out numerical calculations only for Mode 1. Here, it should be noted that the value of N_{in} is 2 for Mode 1 (Fig. 7(b)).

(*) These modes are orthogonal to each other. This is because the directions of the red arrows along the spokes are opposite between these modes. Those of the blue arrows are also opposite. Furthermore, the positions of the green arrows on the rim do not overlap between these modes.

(**) The bright and dark walks correspond to the bright and dark states of the electronic energy states in a molecule, respectively. These states have already been studied with respect to the DPP [9]. Furthermore, a method for building a buffer memory has been proposed by extracting the DPP energy confined in the dark state [10-13].

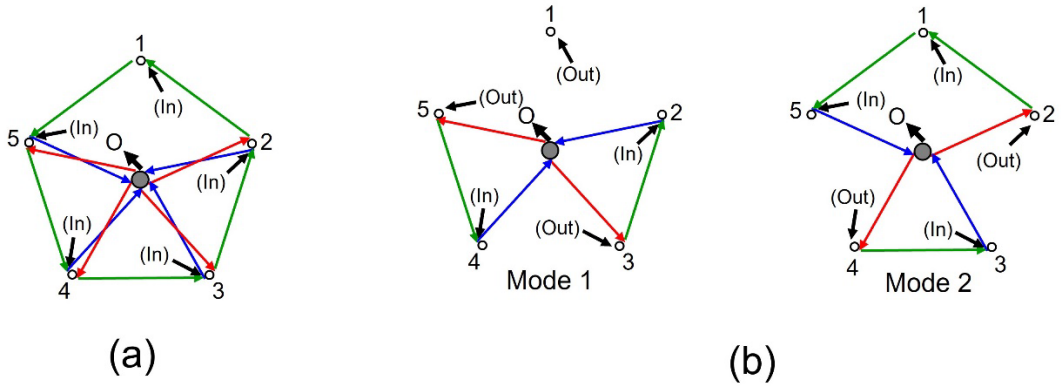

Fig. 7 Arrangement with one disconnected spoke 1.

(a) Schematic explanation of the arrangement. (b) Modes 1 and 2 correspond to the bright and dark walks, respectively. The symbol **(Out)** indicates that the input signal is injected to the ISTs outside the bright walk (Mode 1) and the dark walk (Mode 2).

Figure 8(a) and the first row of Table 2 show the calculated results. They represent the three features below.

1) The stationary value of the OSFR on curve O is smaller than the values of Fig. 2(a) and the first row of Table 1. This is because only the two input signals generate the output signal after transforming through the Mode 1 (bright walk) (N_{in} =2). Since the other three input signals transfer through the Mode 2 (dark walk) (N_{in} =3), they do not generate the output signal.

2) Curves 2 and 4 represent the ISFRs that transfer from ISTs 2 and 4 to the OST, respectively. Since

these input signals are injected into the bright walk of Fig. 7(b) (N_{in} =2), they generate the output signal. Since the distance from IST 2 to the OST is shorter than ~~equal to~~ that from IST 4 (Fig. 8(b)), the ISFR from the former is larger. This distance-dependent feature is ~~in~~consistent with those of Fig. 2(b).

3) Curves 1, 3, and 5 represent the ISFRs that transfer from ISTs 1, 3, and 5 to the OST, respectively. Since these input signals are injected into the dark walk of Fig. 7(b) (N_{in} =3), they are confined in this walk without generating the output signal.

The three features above are inherent to the rotational asymmetric arrangement. In the case of disconnecting the spoke for the IST with other odd number 3 or 5 (IST 3 or 5), the features are equivalent to those of Fig. 8.

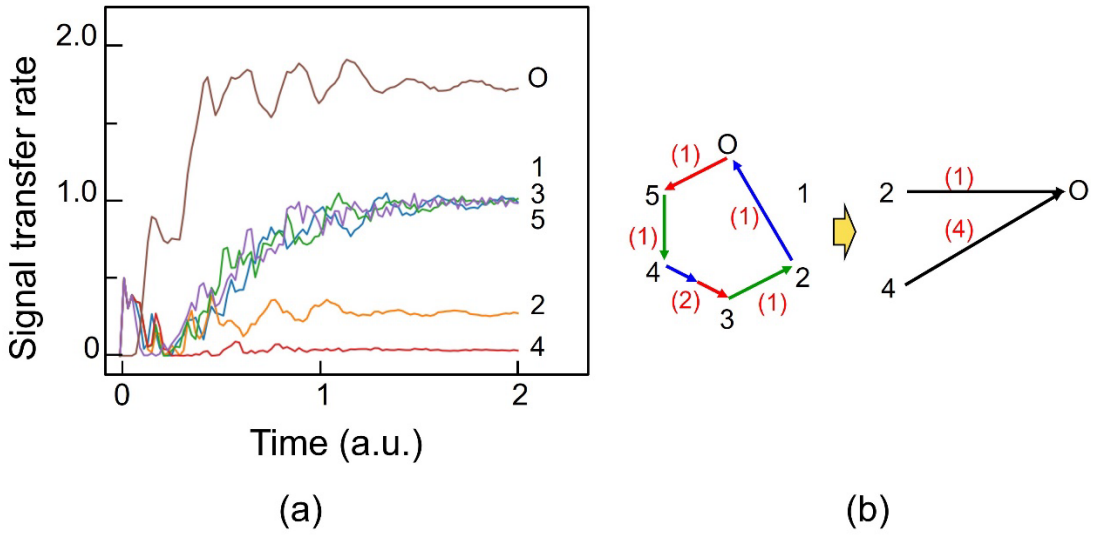

Fig. 8 Results of numerical calculations for the arrangement in Fig. 7.

For captions of (a) and (b), refer to those in Fig. 2.

Table 2 Stationary values of the ISFRs and the OSFRs. The numbers n_{con} of connected spokes are even (=4 and 2).

	n_{con}	The terminal number of the disconnected spokes	ISFR					OSFR
			From terminal 1	From terminal 2	From terminal 3	From terminal 4	From terminal 5	
1	4	1	1.000	0.260	1.000	0.034	1.000	1.706
2	4	2	0.541	0.312	1.000	0.070	1.000	2.077
3	2	1,2,3	1.000	1.000	1.000	0.000	1.000	1.000
4	2	1,3,5	1.000	0.260	0.034	1.000	1.000	1.706
5	2	2,4,5	0.260	0.034	1.000	1.000	1.000	1.706

(2) Figure 9 schematically explains the arrangement in the case of disconnecting the spoke for IST 2. Figure 10 and the second row of Table 2 show the calculated results. They represent features similar to those of Fig. 8. However, the OSFR is larger than that of **(1)** because the value of N_{in} is 3 for Mode 1 (bright walk). Figure 10(a) shows that the ISFRs in the dark walk (curves 3 and 5) are larger than those in the bright walk (curves 1, 2, and 4). However, they are confined in the dark walk without generating the output signal.

In the case of disconnecting the spoke for IST with the other even number 4 (IST 4), the features are equivalent to those of Fig. 10.

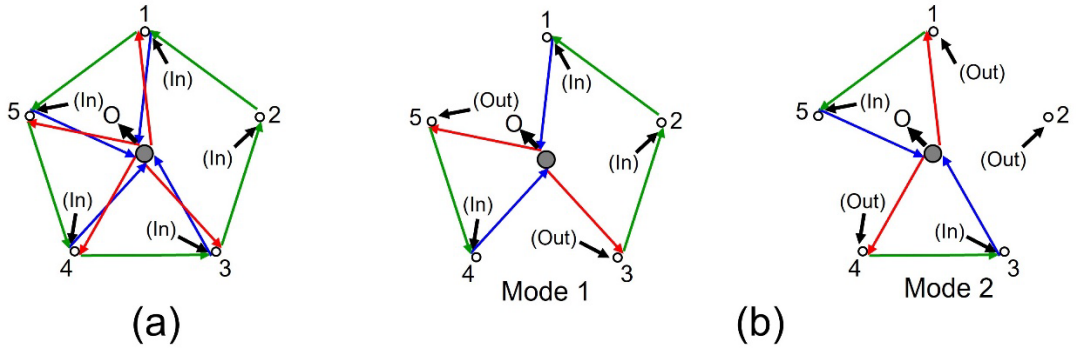

Fig. 9 Arrangement with one disconnected spoke 2.

(a) Schematic explanation of the arrangement. (b) Modes 1 and 2 are the bright and the dark walk, respectively.

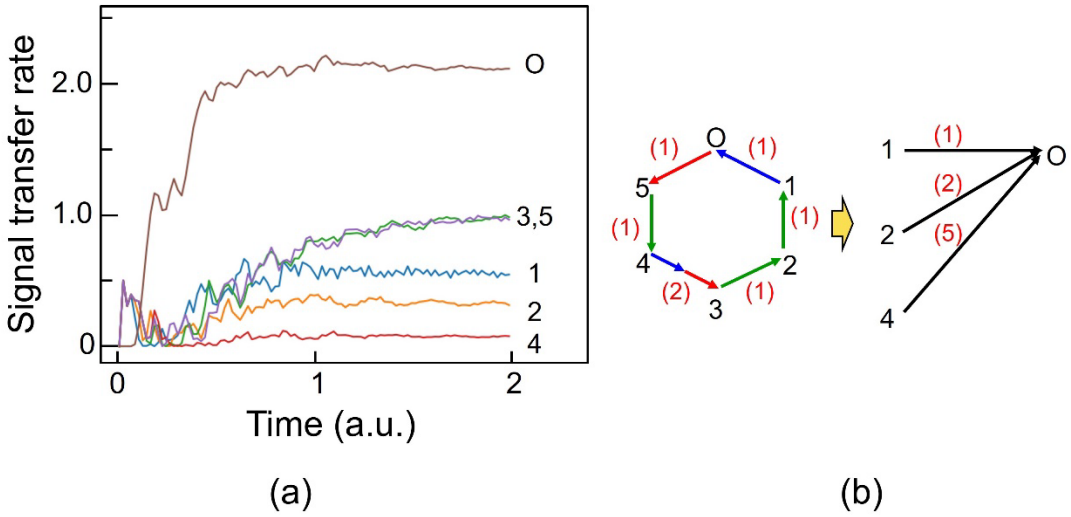

Fig. 10 Results of numerical calculations for the arrangement of Fig. 9.

For captions of (a) and (b), refer to those in Fig. 2.

b. The case of n_{con} =2

The arrangements have the two configurations below.

(1) In the case of the arrangement in which three consecutive spokes 1, 2, and 3 are disconnected (Fig. 11(a)), the value of N_{in} is 1 for Mode 1 (bright walk) (Fig. 11(b)). Figure 12(a) and the third row of

Table 2 show the calculated results for Mode1. Curves 1, 2, 3, and 5 represent the ISFRs to the OST. Since they are in the dark walk, they do not generate the output signal and are confined in the dark walk. Only the input signal 4 is injected into the bright walk. However, the third row of Table 2 indicates that the stationary value of the ISFR to the OST is zero. In the case of the arrangement in which three consecutive spokes 2, 3, and 4 are disconnected (Fig. 11(c)), the value of N_{in} is 4 for Mode 1 (bright walk), as is shown by Fig. 11(d). There are more arrangements in which three consecutive spokes are disconnected, for which the value of N_{in} is also 1 or 4. Their features are equivalent to those of Fig. 11.

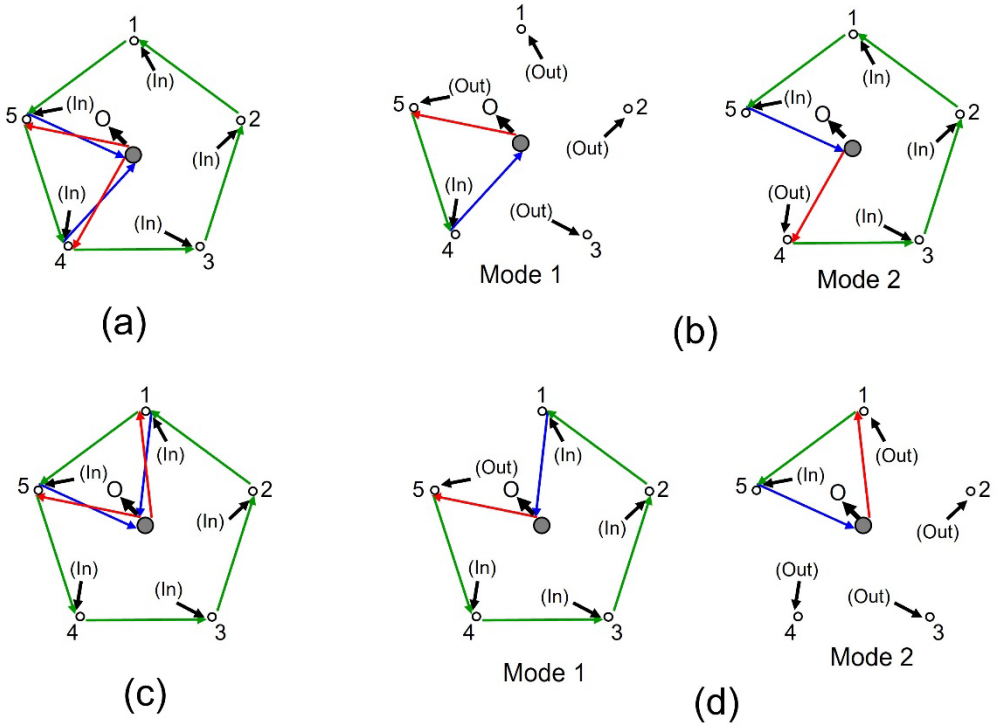

Fig. 11 Arrangement with three disconnected consecutive spokes.

(a) Schematic explanation of the arrangement with the disconnected spokes 1, 2, and 3.

(b) Tw modes for the arrangement (a). Modes 1 and 2 are the bright and dark walks, respectively.

(c) Schematic explanation of the arrangement with the disconnected spokes 2, 3, and 4.

(d) Two modes for the arrangement (a). Modes 1 and 2 are the bright and dark walks, respectively.

(2) Figure 13(a) shows the arrangement in which three spokes 1, 3, and 5 are disconnected. They are not consecutive but there are two connected spokes 2 and 4 between them. Figure 14(a) and the fourth row of Table 2 show the calculated results for Mode 1 (bright walk) (Fig. 13(b)). Since the value of N_{in} is 2 in this Mode 1, the OSFR is larger than that of **(1)** above (N_{in} =1). Other features are equivalent to those of **(1)**. Curves 1, 4 and 5 of Fig. 14(a) represent the ISFRs to the OST. Since ISTs 1, 4, and 5 are in the dark walk, they do not generate the output signal and are confined in the dark walk. ISTs 2 and 3 are in the bright walk. Here, the values of ISTRs 2 and 3 (curves 2 and 3) are smaller than the values of ISTRs 1, 4, and 5 (curves 1, 4, and 5).

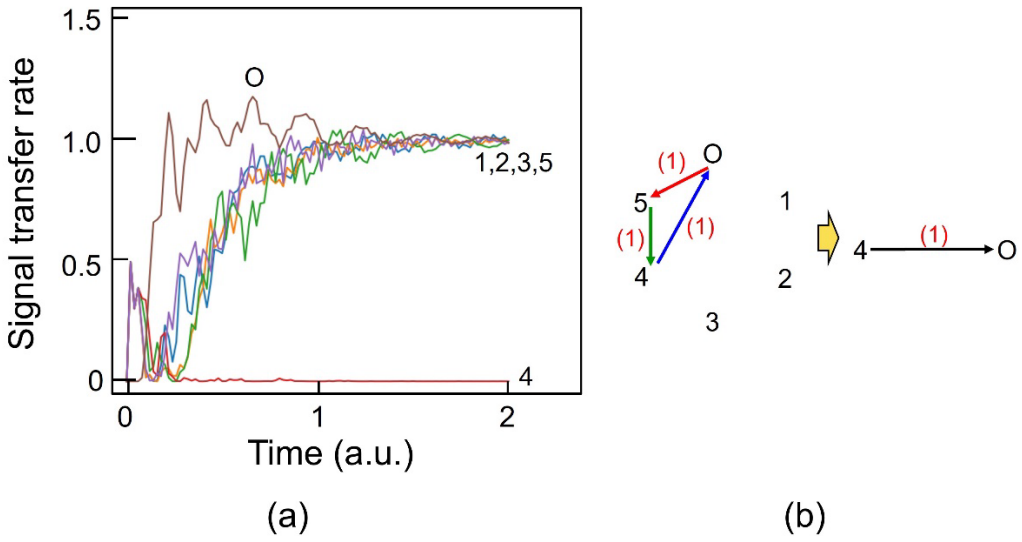

Fig. 12 Results of numerical calculations for the arrangement of Fig. 11(a).

For captions of (a) and (b), refer to those in Fig. 2.

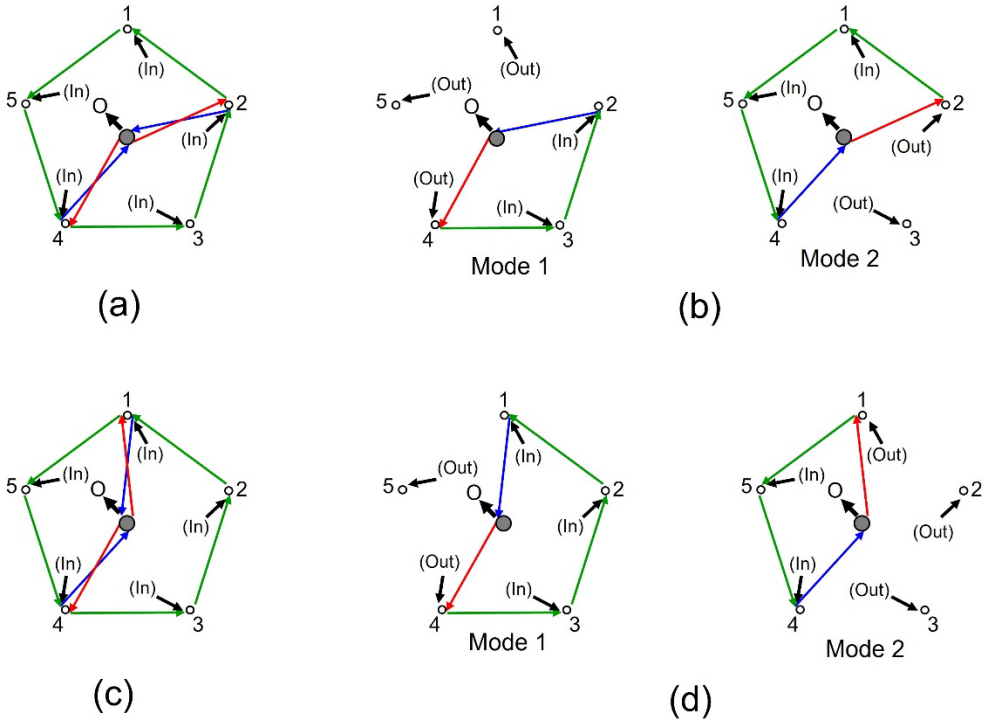

Fig. 13 Arrangement with three disconnected spokes between which two connected spokes exist.

(a) Schematic explanation of the arrangement with the disconnected spokes 1, 3, and 5.

(b) Tw modes for the arrangement (a). Modes 1 and 2 are the bright and dark walks, respectively.

(c) Schematic explanation of the arrangement with the disconnected spokes 2, 3, and 5.

(d) Two modes for the arrangement (a). Modes 1 and 2 are the bright and dark walks, respectively.

Figures 13(c) and (d) show the arrangement in which three spokes 2, 3, and 5 are

disconnected and between which connected spokes 1 and 4 exist. The value of N_{in} is 3 for Mode 1 (bright walk). There are more arrangements in which three spokes are disconnected, as is the case in Figs. 13(a)-(d) (refer to the fifth row of Table 2, as an example). Their values of N_{in} are also 2 or 3, and their features are equivalent to those of Fig. 13.

The third to fifth rows in Table 2 show that the values of the OSFR depend on whether three disconnected spokes are consecutive or not. Table 3 summarizes the relation between the number of connected spokes n_{con} and the value of N_{in} for Mode 1 (bright walk).

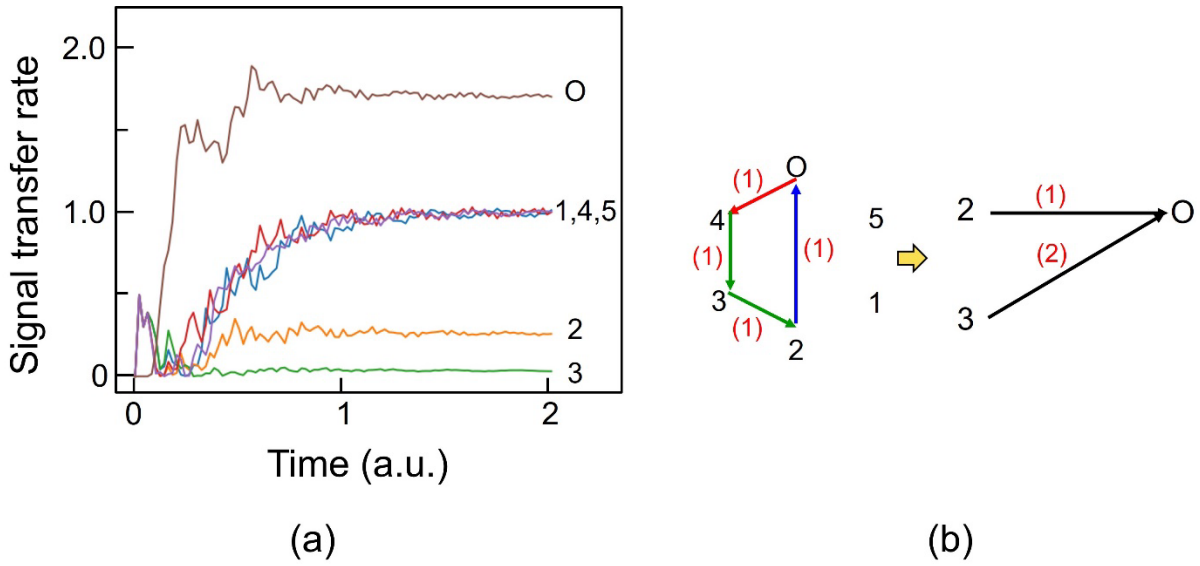

Fig. 14 Results of numerical calculations for the arrangement of Fig. 13(a).
For captions of (a) and (b), refer to those in Fig. 2.

Table 3 Relation between an even number n_{con} (=4 or 2) of connected spokes and the number N_{in} of the input signals injected into the bright walk.

	n_{con}	The terminal number of disconnected spokes	N_{in}
1	4	1	2
2	4	3	2
3	4	5	2
4	4	2	3
5	4	4	3
6	2	1,2,3	1
7	2	2,3,4	4
8	2	3,4,5	4

	n_{con}	The terminal number of disconnected spokes	N_{in}
9	2	4,5,1	1
10	2	5,1,2	1
11	2	1,3,5	2
12	2	2,3,5	3
13	2	1,2,4	2
14	2	2,4,5	2
15	2	1,3,4	3
16	2	2,3,5	3

To summarize **(1)** and **(2)** above, the signal transfer routes are composed of bright and dark

walks when the value of n_{con} is even. If the input signal is injected into the dark walk, it is confined in this walk without generating the output signal. Since only the input signal injected into the bright walk generates the output signal, the stationary value of the OSTR is lower than those in Section 3.1 in which the value of n_{con} is odd.

3.3. Relation between the number of connected spokes and stationary value of the output signal flow rate

Figure 15(a) summarizes the relation between the number n_{con} of connected spokes and the number N_{in} of the input signals injected to the bright walk. The symbol n_{dis} (=5-n_{con}) on the horizontal axis represents the number of disconnected spokes. Figure 15(b) is the relation between N_{in} and the OSFR β_{κ} that was derived from the QW theory [14]. This theory claims that the value of β_{κ} increases with increasing N_{in}, as is shown by Fig. 16. Figure 15(b) was derived by using the values of N_{in} in Fig. 15(a) and the relation in Fig. 16. The values of β_{κ} in Fig. 15(b) agree with the values of the OSFR in Tables 1 and 2.

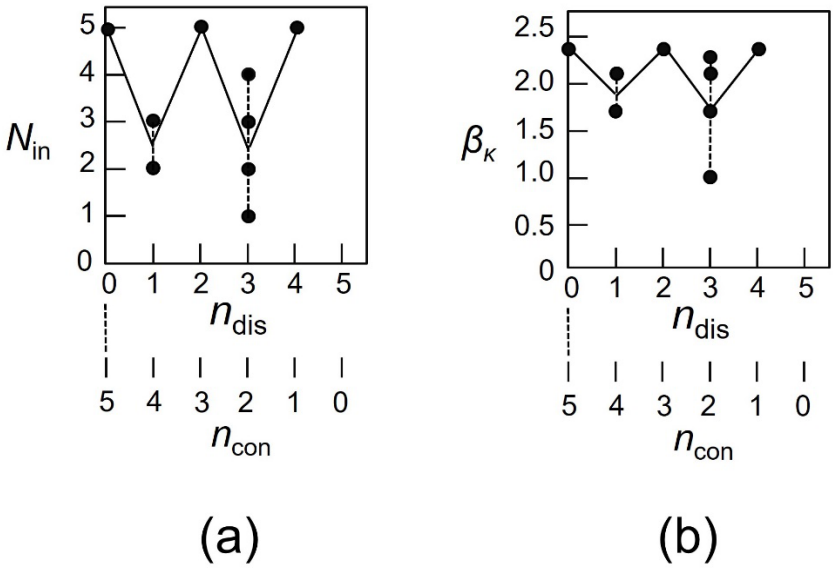

Fig. 15 Dependences of the numerically calculated values on n_{con}.
The symbol n_{dis} (=5-n_{con}) on the horizontal axis represents the number of disconnected spokes.
(a) The number N_{in} of input signals injected inside the bright walk.
(b)The output signal flow rate β_{κ} that was derived from the QW theory [14].

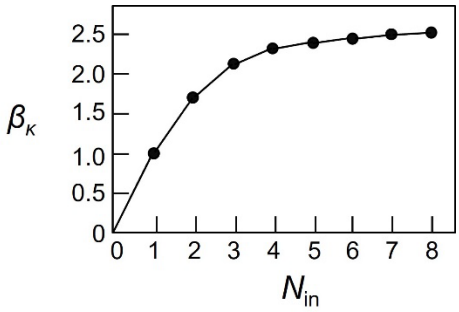

Fig. 16 Relation between N_{in} and β_K [14].

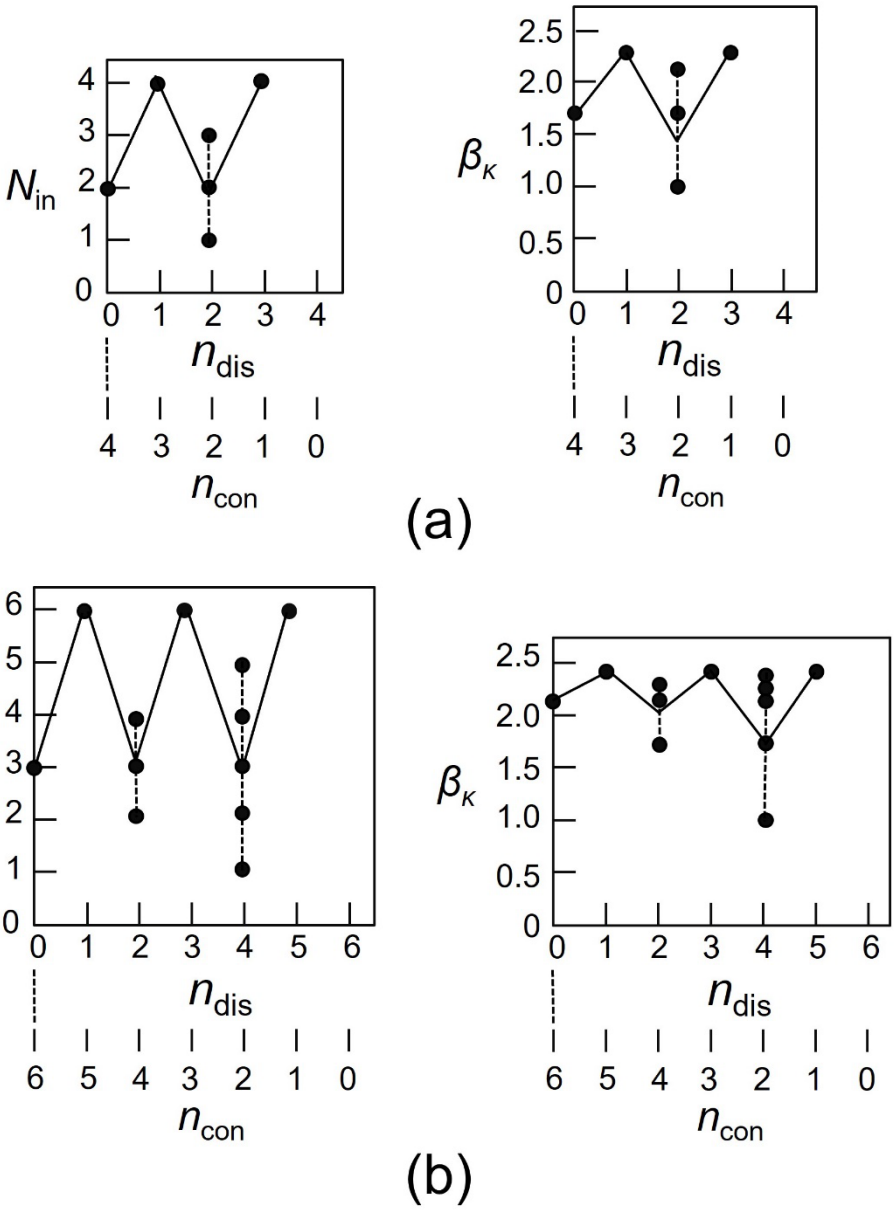

Fig. 17 Dependences of the results of numerically calculated values on n_{con}.
(a) and (b) are for tetrahedral and hexagonal arrangements, respectively.

Figures 15(a) and (b) show that the values of N_{in} and β_{κ} vary periodically, and are due to the following dependences **(1)** and **(2)** on n_{con} :

(1) In the case where the number n_{con} of connected spokes is odd, the signal transfer routes correspond to the bright walk, and thus, N_{in} =5 for the cases of n_{con} =1, 3, and 5. This means that the bright walks are triply degenerate.

(2) In the case where the number n_{con} of connected spokes is even (=2 or 4), the number N_{in} of the bright walk is smaller than 5, which is due to the existence of the dark walk. Thus, the OSFR is smaller than that of **(1)** because the input signals in the dark walk do not generate the output signal.

Figures 17(a) and (b) show the results of numerical calculations for tetrahedral and hexagonal arrangements, respectively. Their periodic variation features are consistent with those of Fig. 15, by which it was proved that these features are independent of the number of NP_I on the rim of the wheel. However, it should be noted that the periodically varying features of Fig. 17 are in anti-phase with respect to those of Fig. 15.

4. Summary

This paper reported that the DPP energy transfer routes are triply degenerate bright walks in the case where the number n_{con} of connected spokes is odd. Thus, even if some spokes are disconnected, the stationary values of the OSFR are kept equal to that of the arrangement without any disconnection. Such an n_{con} -independent feature is consistent with the results of preliminary numerical calculations [8].

In the case where the number n_{con} of connected spokes is even, the energy transfer routes are decomposed into bright and dark walks. Since some input signals are injected into the dark walk, the value of the OSFR is smaller than that of the case of the odd number of the connected spokes above.

The degeneracy in the bright walk and the existence of the dark walk above were found not only in the pentagonal arrangement but also in other polygonal arrangements, which showed that their features are independent of the number of NP_I on the rim of the wheel of these arrangements.

It will be interesting to find a method of extracting the confined signal from the dark walk to the outer system in order to use it in a variety of applications.

References

[1] H. Sakuma, I. Ojima, M. Ohtsu, and T. Kawazoe, Drastic advancement in nanophotonics achieved by a new dressed photon study, “JEOS-RP (2021) **17**: 28.

[2] H. Sakuma, I. Ojima, and M. Ohtsu, “Perspective on an Emerging Frontier of Nanoscience Opened up by Dressed Photon Studies,” *Nanoarchitectonics*, Vol. 5, Issue 1 (2024) pp.1-23.

[3] M. Ohtsu, *Dressed Photons*, Springer

[4] M. Ohtsu, Silicon LED and Lasers, Springer

[5] M. Naruse, T. Kawazoe, R. Ohta, W. Nomura, M. Ohtsu, "Optimal mixture of randomly dispersed quantum dots for

optical excitation transfer via optical near-field interactions," Phys. Rev. B **80**, 125325 (2009)

[6] M. Ohtsu, E. Segawa, K. Yuki, and S. Saito, "Quantum walk analyses of the off-shell scientific features of dressed-photon–phonon transfers among a small number of nanometer-sized particles," *Off-shell Archive* (July, 2024) Offshell: 2407O.001.v1. **DOI** 10.14939/2407O.001.v1

[7] M. Ohtsu and H. Sakuma, *Dressed Photon to Revolutionize Modern Physics*, Springer, Heidelberg (to be published in 2025) Section 4.1.

[8] M. Naruse, K. Leibnitz, F. Peper, N. Tate, W. Nomura, T. Kawazoe, M. Murata, M. Ohtsu, "Autonomy in excitation transfer via optical near-field interactions and its implications for information networking," Nano Commun. Networks **2**, (2011) pp. 189-195.

[9] M. Ohtsu, *Dressed Photons*, Springer, Heidelberg (2014) pp.38-39

[10] M. Ohtsu, *Dressed Photons*, Springer, Heidelberg (2014) pp.115-117.

[11] S. Sangu, K. Kobayashi, M. Ohtsu, IEICE Trans. Electron., **E88-C**, 1824 (2005)

[12] M.Ohtsu, "Novel functions and prominent performance of nanometric optical devices made possible by dressed photons," ," *Off-shell Archive* (April, 2019) Offshell: 1904O.001.v1. **DOI** 10.14939/1904O.001.v1

[13] M. Ohtsu, *Off-shell Applications in Nanophotonics*, Elsevier, Amsterdam (2021) pp.58-59.

[14] E. Segawa, S. Saito, K. Yuki, and M. Ohtsu, "Quantum walk simulation of energy transport problem for dressed photon on wheel graph," Abstracts of the 84th Jpn. Soc. Appl. Phys. Autumn Meeting, September 19-23, 2023 (Kumamoto Castle Hall and Online meeting), paper number 22p-A310-6.